Tensile Strength of Unsaturated Sand

Ning Lu, F.ASCE[1]; Tae-Hyung Kim, M.ASCE[2]; Stein Sture, F.ASCE[3]; and William J. Likos, M.ASCE[4]

Abstract: A theory that accurately describes tensile strength of wet sand is presented. A closed form expression for tensile strength unifies tensile strength characteristics in all three water retention regimes: pendular, funicular, and capillary. Tensile strength characteristically increases as soil water content increases in the pendular regime, reaches a peak in the funicular regime, and reduces with a continuing water content increase in the capillary regime. Three parameters are employed in the theory: internal friction angle (at low normal stress) ϕ_l, the inverse value of the air-entry pressure α, and the pore size spectrum parameter n. The magnitude of peak tensile strength is dominantly controlled by the α parameter. The saturation at which peak tensile strength occurs only depends on the pore size spectrum parameter n. The closed form expression accords well with experimental water retention and tensile strength data for different sands.

DOI: 10.1061/(ASCE)EM.1943-7889.0000054

CE Database subject headings: Tensile strength; Sand, soil type; Unsaturated soil; Soil water; Soil suction; Effective stress.

Introduction

Tensile strength of granular media is often used as an indication for a material's capability to sustain an external tensile stress without breaking. For materials with strong bonding forces among the grains, such as concrete or rock, tensile strength can be experimentally obtained by applying a uniaxial extensional stress on a rod-shaped specimen until failure. For granular materials with weak intergranular bonding forces such as soils, a special apparatus with typically nonrod shaped specimen is needed (Bishop and Garga 1969; Al-Hussaini and Townsend 1974; Kim and Hwang 2003). For soils that are either completely dry or fully saturated, tensile strength is often considered as a material constant or part of shear strength. For soils under partially saturated conditions, tensile strength is not a constant, but rather depends on degree of saturation or pore water suction (e.g., Lu et al. 2007).

Because tensile strength generally varies greatly with saturation and its magnitude could be on the order of several kPa for sandy soils (e.g., Lu et al. 2005) or several hundreds of kPa for clayey soils (e.g., Zeh and Witt 2007), it may have profound impacts on the performance and stability of many earthworks. Most existing theories for predicting the tensile strength of moist granular material are derived by considering intergranular forces for idealized particles and packing geometries and are only applicable over a limited range of saturation. For example, numerous models have been developed to quantify liquid bridge forces developed between particles in the pendular regime for simplified two-particle systems represented by smooth spheres, rough spheres, parallel plates, and other such geometries (e.g., Fisher 1926; Dallavalle 1943; Ingles 1962; Blight 1967; Sparks 1963; Mehrotra and Sastry 1980; Schubert 1982; Cho and Santamarina 2001; Likos and Lu 2004). Common among these models, however, is the requirement for assumptions or explicit knowledge of particle shape, surface roughness, size, separation distance, surface tension, and solid-liquid contact angle. Rumpf (1961) presented a model for predicting the corresponding tensile strength of moist particle agglomerates in the pendular regime by upscaling a theorized liquid bridge force for monosized spherical particles under the assumption that the particles are uniformly distributed and compacted to some uniform porosity. Schubert (1982) extended this model into the funicular and capillary regimes by using a normalized degree of saturation to superimpose Rumpf's interparticle stress in the pendular regime with the stress directly arising from negative pore pressure in saturated pockets of pores. While the Rumpf-Schubert model captures some of the aspects of soil tensile strength as a function of saturation (Kim 2001), the idealizations and assumptions that are required have limited its theoretical and practical applications.

Here we develop a theory for the tensile strength of moist granular media derived by considering the suction stress of Lu and Likos (2006), defined as the isotropic interparticle stress arising from capillary mechanisms in unsaturated soil. Apparent cohesion widely recognized to characterize the behavior of unsaturated soil is illustrated to be the mobilization of suction stress to shear resistance. Experimental results from direct tension tests are considered to show that the tensile strength of moist granular specimens can be accurately predicted using the suction stress concept if the frictional characteristics (ϕ) and soil-water characteristic curve (SWCC) of the material are known.

Dry and Moist Sand with Mohr-Coulomb Behavior

For most practical engineering problems dealing with sandy soil and stress levels on the order of tens to hundreds of kPa, the

[1]Professor, Div. of Engineering, Colorado School of Mines, Golden, CO 80401 (corresponding author). E-mail: ninglu@mines.edu

[2]Assistant Professor, Dept. of Civil Engineering, Korea Maritime Univ., Busan 606-791, Korea.

[3]Professor and Vice Chancellor for Research, Univ. of Colorado–Boulder, the Regent Administrative Center, Boulder, CO 80309.

[4]Associate Professor, Dept. of Civil and Environmental Engineering, Univ. of Missouri–Columbia, Columbia, MO 65211.

Note. This manuscript was submitted on July 24, 2008; approved on April 24, 2009; published online on April 29, 2009. Discussion period open until May 1, 2010; separate discussions must be submitted for individual papers. This paper is part of the ***Journal of Engineering Mechanics***, Vol. 135, No. 12, December 1, 2009. ©ASCE, ISSN 0733-9399/2009/12-1410–1419/$25.00.

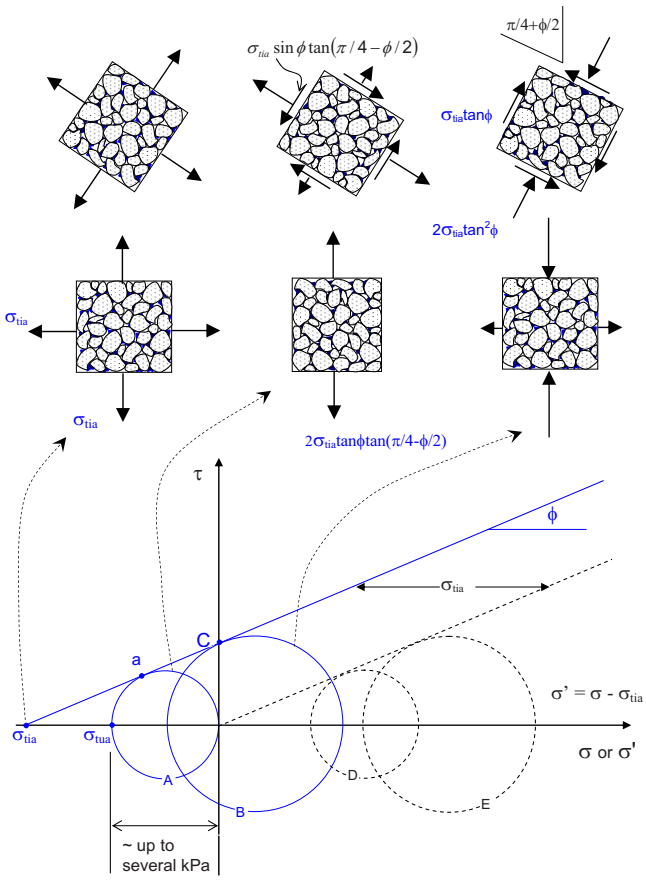

Fig. 1. Conceptual illustration of state of stress for isotropic tensile strength, uniaxial tensile strength, and apparent cohesion for M-C failure. Solid curve and circle are for the total stress representation whereas dashed curve and circle are for the effective stress representation.

Mohr-Coulomb (M-C) failure criterion is widely employed. The criterion, as graphically illustrated in Fig. 1, hypothesizes the shear strength of soil as a linear function of normal stress. For dry sand, it states that for any point in any direction in the soil domain, the failure or limit state will be reached if the ratio of shear stress to normal stress reaches a critical value tan ϕ

$$\tau = \sigma \tan \phi \tag{1}$$

In the following, the sign convention widely used in soil mechanics will be used. Thus, compressive stress is positive and tensile stress is negative.

For moist or unsaturated sand, interparticle liquid bridges and saturated pockets of pore water under negative pressure provide an additional component of bonding stress. In the case of homogeneous and isotropic sand, as shown in the top left in Fig. 1, this bonding stress is the source for isotropic tensile strength σ_{tia}, which is also shown as a point on the far left of the normal stress axis. Under such conditions, there is no shear stress at any point in any direction, and failure occurs only when the applied external stress reaches the bonding strength (or tensile strength) provided by capillarity. This strength exists with or without presence of the external stresses. Because no shear stress develops when soil fails under isotropic tensile stress, the isotropic tensile strength of soil is independent of the internal friction angle.

In contrast to isotropic tensile strength, uniaxial tensile strength σ_{tua} may be defined for the case where a soil element fails under tensile stress applied normal to one principal plane, with zero stress applied to corresponding orthogonal planes. This is the tensile strength measured via various forms of direct tension tests in the literature (e.g., Bishop and Garga 1969; Al-Hussaini and Townsend 1974; Perkins 1991; Kim and Hwang 2003; Lu et al. 2005), although it is unlikely that truly uniaxial conditions are actually maintained for specimens initially compacted into confining molds.

If it is assumed that the ratio of shear stress to normal stress in the tensile stress regime remains the same as in the compressive stress regime, i.e., tan ϕ, then uniaxial tensile strength σ_{tua}, can be logically considered as the mobilization of isotropic bonding stress when the maximum principal stress remains zero. This state of stress is depicted as Circle A in Fig. 1 and is illustrated for a corresponding soil element in the top middle portion of the figure. In other words, failure occurs not because the applied stress reaches the bonding strength, but because the ratio of shear stress to normal stress at point *a* reaches tan ϕ. Thus, the uniaxial tensile strength measured in typical experiments is actually a measurement of frictional strength resulting from the mobilization of isotropic bonding stress. As depicted in the top middle in Fig. 1, the magnitude of mobilized shear strength at this state is equal to $\sin\phi\ \tan(\pi/4-\phi/2)\sigma_{tia}$.

The maximum amount of mobilized shear strength due to the isotropic bonding stress is the interception of the M-C criterion to the shear stress axis (Point C), and is commonly called apparent cohesion in the literature. Here, the corresponding state of stress is depicted as Circle B in Fig. 1 and for the soil element in the top right. As shown, *C* is a shear stress, rather than a normal stress and thus the name "apparent cohesion" is misleading. On the other hand, the isotropic tensile strength is indeed a direct reflection of intergranular bonding stress, which is closer to the meaning of the phrase "apparent cohesion."

Mathematical relationships among isotropic tensile strength (σ_{tia}), apparent cohesion (C), and uniaxial tensile strength (σ_{tua}) can be established by considering the geometry on Fig. 1 as

$$\frac{C}{\sigma_{tia}} = -\tan\phi \tag{2a}$$

$$\frac{C}{\sigma_{tua}} = -\frac{1}{2\tan\left(\frac{\pi}{4}-\frac{\phi}{2}\right)} \tag{2b}$$

$$\frac{\sigma_{tua}}{\sigma_{tia}} = 2\tan\phi\tan\left(\frac{\pi}{4}-\frac{\phi}{2}\right) \tag{2c}$$

Fig. 2 illustrates the above relationships. As indicated, the efficiency with which the external stress mobilizes isotropic bonding stress or tensile strength σ_{tia} to shear strength C increases from less than 40% at a friction angle of 20° to over 270% at a friction angle of 70°. At a friction angle of 45°, the mobilized shear strength C is equal to the isotropic tensile strength. The ability of sand to mobilize isotropic bonding stress to uniaxial tensile strength varies from 51% at a friction angle of 20° to 97% at a friction angle of 70°. This suggests that uniaxial tensile strength, such as that measured in ideal direct tension tests, will be less than or equal to the isotropic tensile strength for M-C materials.

The Circle B touching the M-C envelope on the shear stress axis at C has some interesting features. First, it can only be attained for the unique pair of principal stresses shown in the top right of Fig. 1. The maximum principal stress is compressive and

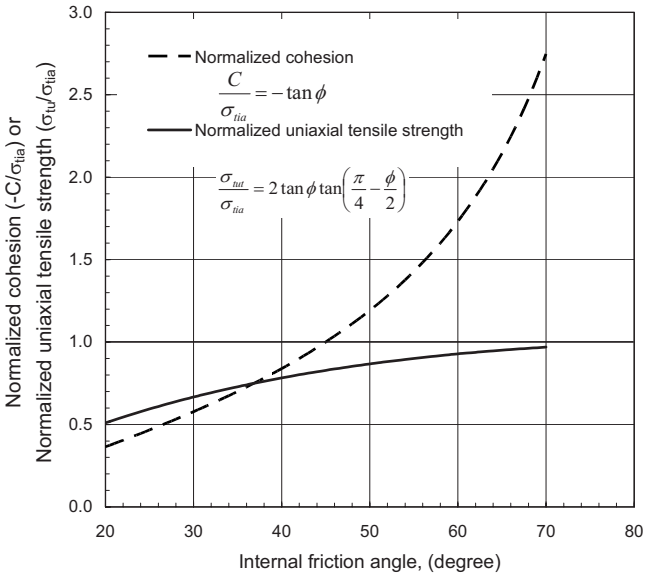

Fig. 2. Illustration of the abilities of uniaxial tensile strength and apparent cohesion in mobilizing isotropic tensile stress into shear stress as functions of friction angle

the minimum principal stress is tensile. The ratio of the minimum principal stress to the maximum principal stress is equal to the negative coefficient of active earth pressure $\tan^2(\pi/4-\phi/2)$. There exists only a pair of parallel planes where zero normal stress occurs at $\pi/4+\phi/2$ from the plane of the maximum principal stress. However, on the planes orthogonal to this pure shear plane, there is additional compressive normal stress equal to $2\sigma_{tia}\tan^2\phi$.

Isotropic tensile strength has been used to quantify the differences observed in the behavior of moist and dry granular soil. This is illustrated by the rightward shift of the failure envelope in Fig. 1. Lu and Likos (2006) defined the isotropic tensile strength as a part of effective stress called "suction stress." Much like positive pore water pressure in saturated soil, suction stress may be considered as additive with total stress to define an effective stress, thereby allowing unsaturated soils to be considered within Terzaghi's conventional effective stress framework. Because suction stress is generally tensile, it increases the effective stress under unsaturated conditions. According to Lu and Likos (2006), suction stress has four components arising from various physical and physico-chemical mechanims: van der Waals attractive forces, electric double layer forces, tensile pore water pressure, and surface tension. For unsaturated fine-grained materials such as clay, all four components are important to consider over a wide range of saturation. For unsaturated coarse-grained materials such as sand, the latter two—tensile pore water pressure and surface tension—dominate the generation of suction stress. Under the framework of the suction stress concept, these stress mechanisms can be unified and the effective stress for both saturated and unsaturated soil can be cast in one unified form

$$\sigma' = \sigma - u_a - \sigma^s = \sigma - u_a - f(u_a - u_w) = \sigma - u_a - f(S) \qquad (3)$$

where u_a=pore air pressure; u_w=pore water pressure; S=degree of saturation; and σ^s=suction stress. As illustrated by the dashed Mohr Circles D and E in Fig. 1, moist sand under conditions of isotropic tensile stress due to capillarity can be treated as equivalent dry sand with no isotropic tensile strength (cohesion) if the above generalized effective stress is employed.

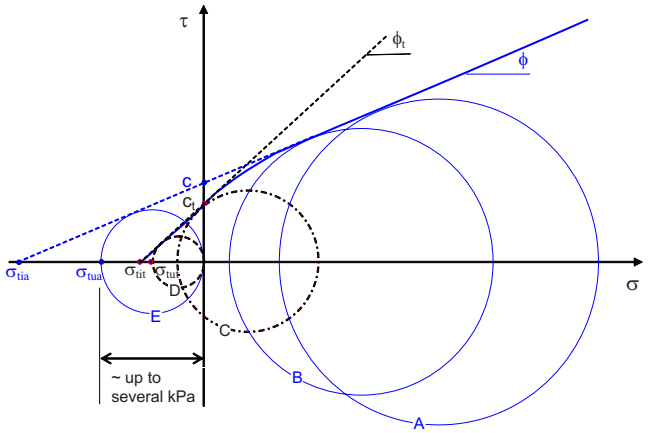

Fig. 3. Conceptual illustration of the proposed theory for non-M-C failure of sand in tensile stress regime

Dry and Moist Sand with Non-Mohr-Coulomb Behavior

Depending on relative density, stress history, and the magnitude of stress, the failure behavior of sand may not follow M-C frictional behavior. For stress magnitudes in the large compressive range, say from tens to hundreds of kPa and as illustrated by Circles A and B in Fig. 3, the M-C criterion is generally an adequate representation for the shear strength behavior of sand. However, experimental evidence (e.g., Maksimovic 1989, 1996; Sture et al. 1998; Kim 2001) has shown that for small magnitudes of compressive stress, say less than tens of kPa, and particularly in the tensile stress regime, the M-C criterion often cannot be accurately used for representing the shear strength behavior of sand.

Illustrated in Fig. 3 is the conceptual behavior of shear strength in those low stress regimes. A nonlinear relationship between shear strength and normal stress is often the case if the applied normal stress is less than several kPa. The ratio of shear stress to normal stress typically increases significantly as the normal stress decreases. For example, Kim (2001) reported that for dry clean Ottawa sand (F-75), friction angle is 23° within the range of normal stress from 0.5 kPa to 1.0 kPa, but increases progressively to 28° within the range of normal stress from 0.25 kPa to 0.5 kPa, and to 47° for normal stress from 0.1 kPa to 0.25 kPa. Friction angles as high as 70° for clean sand at small normal stress levels have also been reported (Sture et al. 1998).

Higher friction angles measured at low normal stresses for sand is mainly explained by the interlocking mechanism. Even for dry sand, small apparent cohesion, on the order of several hundred to several thousands of Pa, is often observed depending on the stress range used to infer apparent cohesion.

For sand behavior under small compression regimes, such as under low or zero gravity, or under undergoing tensile failure, such as tensile zones in the crest area of hillslopes or behind retaining walls, it is important to consider the aforementioned nonlinear behavior. There are also additional applications involving moist granular media under tensile stress conditions, such as material processing, manufacturing, and transporting, and tensile failure in sandy soil under shallow ground environment.

As illustrated in Fig. 3, linear shear strength behavior in the tensile regime may be assumed to arrive at a closed form expression for the uniaxial tensile strength. The nonlinear behavior in

the compression regime is recognized to define the friction angle near zero normal stress, and is extended to define the linear portion in the tensile regime. The physical justification for this assumption will be discussed later.

It should be recognized that most laboratory tensile strength test techniques are neither measuring isotropic tensile strength nor uniaxial tensile strength, although most tensile strength measurements are more close to the uniaxial tensile strength condition. Note from Fig. 2 that as the friction angle becomes higher, the difference between isotropic tensile strength and uniaxial tensile strength becomes smaller. For example, if the friction angle at low normal stress level is 50°, the uniaxial tensile strength is 87% of the isotropic tensile strength. If the friction angle is 60°, the uniaxial tensile strength is 93% of the isotropic tensile strength.

The mathematical relationship among isotropic tensile strength, apparent cohesion, and uniaxial tensile strength can be established the same way as the case for linear M-C materials by consideration of geometry as

$$\frac{C_t}{\sigma_{\text{tit}}} = -\tan \phi_t \tag{4a}$$

$$\frac{C_t}{\sigma_{\text{tut}}} = -\frac{1}{2\tan\left(\frac{\pi}{4} - \frac{\phi_t}{2}\right)} \tag{4b}$$

$$\frac{\sigma_{\text{tut}}}{\sigma_{\text{tit}}} = 2\tan \phi_t \tan\left(\frac{\pi}{4} - \frac{\phi_t}{2}\right) \tag{4c}$$

where the subscript t=realistic values for apparent cohesion and friction angle under the nonlinear failure envelope.

The necessity to consider the non-M-C behavior can be examined by considering the ratio of Eq. (2*c*) to Eq. (4*c*)

$$\frac{\sigma_{\text{tut}}}{\sigma_{\text{tua}}} = \frac{C_t}{C}\frac{\tan\left(\frac{\pi}{4} - \frac{\phi_t}{2}\right)}{\tan\left(\frac{\pi}{4} - \frac{\phi}{2}\right)} \tag{5}$$

Considering moist Ottawa sand (F-75) at a degree of saturation of 2% as an example, Kim (2001) reported that

$$C_t = 263 \text{ (Pa) and } \phi_t = 49° \quad \text{for} \quad 100 \leqslant \sigma \leqslant 250 \text{ (Pa)}$$

$$C = 382 \text{ (Pa) and } \phi = 34° \quad \text{for} \quad 500 \leqslant \sigma \leqslant 1{,}000 \text{ (Pa)}$$

which leads to over 100% relative error in the uniaxial tensile strength, i.e.

$$\frac{\sigma_{\text{tut}}}{\sigma_{\text{tua}}} = \frac{C_t}{C}\frac{\tan\left(\frac{\pi}{4} - \frac{\phi_t}{2}\right)}{\tan\left(\frac{\pi}{4} - \frac{\phi}{2}\right)} = \frac{263}{382}\frac{\tan(45 - 24.5)}{\tan(45 - 17)} = 0.48$$

However, the difference between the uniaxial tensile strength σ_{tut} and the isotropic tensile strength σ_{tit}, as argued earlier, becomes smaller and smaller as the friction angle becomes higher and higher. This is particularly true for friction angle greater than 50°, as shown in Fig. 2. The difference is less than 10%. This point serves as a justification for the linear yield envelope assumption in the tensile regime.

Relationship between Suction and Tensile Strength

As proposed by Lu and Likos (2004,2006), suction stress can be quantitatively expressed in terms of soil suction under field conditions in the following form:

$$\sigma^s = u_w \quad \text{for} \quad u_a - u_w \leqslant 0$$

$$\sigma^s = -(u_a - u_w)\{+[\alpha(u_a - u_w)]^n\}^{1/n-1} \quad \text{for} \quad u_a - u_w \geqslant 0 \tag{6}$$

or in term of the equivalent degree of saturation

$$\sigma^s = u_w \quad \text{for} \quad u_a - u_w \leqslant 0$$

$$\sigma^s = -\frac{S_e}{\alpha}\left(S_e^{n/(1-n)} - 1\right)^{1/n} \quad \text{for} \quad u_a - u_w \geqslant 0 \tag{7}$$

where α=inverse value of the air-entry pressure; n=pore size spectrum number; and S_e=equivalent degree of saturation. The parameter n varies between 2 and 8.5 (e.g., Lu and Likos 2004) with values deviating from 1 indicate wider pore size distribution. Equivalent saturation is defined as degree of saturation normalized by the residual saturation S_r as follows:

$$S_e = \frac{S - S_r}{1 - S_r} \tag{8}$$

The relation between soil suction and the equivalent degree of saturation (i.e., the SWCC) by the model of van Genuchten (1980) is

$$S_e = \{+[\alpha(u_a - u_w)]^n\}^{1/(n-1)} \tag{9}$$

Since suction stress defined by Lu and Likos (2006) is the isotropic tensile stress that can be conceptualized as the isotropic tensile strength, Eq. (6) or Eq. (7) can be directly used to estimate uniaxial tensile strength. Substituting Eq. (6) or Eq. (7) into Eq. (4*c*) leads to expressions for the uniaxial tensile strength in its absolute value hereafter in two forms

$$\sigma_{\text{tut}} = 2\tan \phi_t \tan\left(\frac{\pi}{4} - \frac{\phi_t}{2}\right)(u_a - u_w)\{+[\alpha(u_a - u_w)]^n\}^{1/(n-1)} \tag{10a}$$

$$\sigma_{\text{tut}} = 2\tan \phi_t \tan\left(\frac{\pi}{4} - \frac{\phi_t}{2}\right)\frac{S_e}{\alpha}\left[S_e^{n/(1-n)} - 1\right]^{1/n} \tag{10b}$$

Thus, the above two equations may be used to predict the unixial tensile strength of unsaturated soil as a function of suction or degree of saturation if the internal friction angle and SWCC (α and n) are known.

Characteristics of Tensile Strength of Moist Sand

It is well known that moist sand generally exhibits cohesion with a magnitude dependent on the degree of wetness or saturation, particle size, particle-size distribution, and porosity. Perhaps the most striking and persistent characteristic of moist sand behavior is the nonlinear dependence of tensile strength on saturation or soil suction. Qualitatively, dry sand has minimal tensile strength even though the interlocking of the sand could be strong. As sand progressively wets toward full saturation, the degree of saturation increases, and soil suction reduces. However, the bonding stress (isotropic tensile strength) will first increase up to a maximum value depending on particle size and porosity, followed by a re-

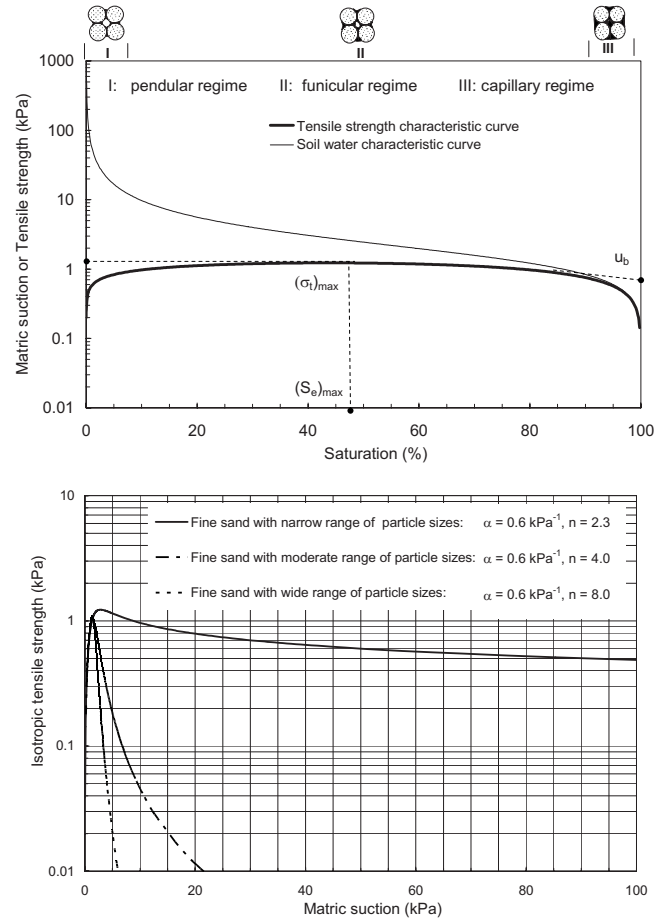

Fig. 4. Illustration of the characteristics of tensile strength of sand: (a) interrelationship between soil water retention curve and tensile strength characteristic curve for over the entire saturation range; (b) tensile strength of fine sand as a function of soil suction for different pore size distributions

duction to zero near saturation or when the sand is sufficiently wet. A conceptual illustration of such up-and-down behavior of tensile strength of sand is shown in Fig. 4(a).

Because capillary water can be retained in three distinct regimes—pendular, funicular, and capillary regimes—theoretical formulation of soil tensile strength has been challenging. Nearly all the existing theories are based on consideration of water retention and capillary force interactions between idealized two-particle pairs in the pendular regime, and thus cannot accurately describe tensile strength for multiparticle systems in the funicular regime. For typical sand, the pendular regime represents up to about 20% saturation, the funicular regime between approximately 20 and 90%, and capillary regime between approximately 90 and 100%. Consequently, while most existing theories can quantitatively predict the magnitude of tensile strength in the pendular regime, few of them can accurately predict the occurrence of the maximum tensile strength or the variation of tensile strength in the funicular and capillary regimes. To date, no experimentally validated closed form expression has been proposed.

The theory presented in this paper [Eq. (10)] can be used to predict tensile strength behavior in all three water retention regimes. This may be illustrated by first considering three idealized cases. Fig. 4(b) illustrates the tensile strength of three hypothetical fine sands as a function of soil suction described by Eq. (10*a*). All three fine sands have the same air-entry pressure of 1.67 kPa, which will cause 16.7 cm of capillary fringe above the water table under hydrostatic field conditions. For the fine sand with a narrow range of particle sizes, the pore size distribution is also narrow ($n=2.3$). The maximum tensile strength is 1.23 kPa, which occurs at matric suction of 2.81 kPa or 43.6% of saturation (not shown in the figure). Tensile strength reduces relatively slowly as matric suction increases after passing the peak value. At matric suction of 100 kPa (0.5% of saturation), tensile strength still sustains about 0.48 kPa. For the fine sand with a moderate particle size and pore-size distribution ($n=4$), the maximum tensile strength is 1.03 kPa, which occurs at matric suction of 1.40 kPa or 73.8% of saturation. Tensile strength reduces quickly as matric suction increases after passing the peak strength. Tensile strength is 0.01 kPa at matric suction of 22 kPa (or saturation of 0.04%). Finally, for the fine sand with a wide particle-size and pore-size distribution ($n=8$), the maximum tensile strength is 1.10 kPa, which occurs at matric suction of 1.32 kPa or 83.0% of saturation. Tensile strength decreases very rapidly after the peak value, and it reaches 0.01 kPa at matric suction of 6 kPa (or saturation of 0.03%). It can be drawn from these three hypothetical cases that the magnitude of tensile strength is greatly controlled by the air-entry pressure parameter α, the peak tensile strengths occurred at very similar matric suction values, but quite different saturations [43.6, 74.8, and 83.0% calculated from Eq. (10*b*)] for these three sands.

Accurate prediction of the maximum tensile strength and its occurrence may also be derived from Eq. (10*a*) or Eq. (10*b*). Taking the derivative of Eq. (10*b*), for example, with respect to the equivalent degree of saturation and setting it to be zero leads to the maximum magnitude of uniaxial tensile strength

$$(\sigma_{tut})_{max} = \frac{2}{\alpha}\tan\phi_t \tan\left(\frac{\pi}{4} - \frac{\phi_t}{2}\right)\left(\frac{1-n}{2-n}\right)^{(1-n)/n}\left(\frac{1}{2-n}\right)^{l/n} \tag{11}$$

The corresponding degree of saturation is

$$(S_e)_{max} = \left(\frac{1-n}{2-n}\right)^{(1-n)/n} \tag{12}$$

where n is identified to be valid for greater than 2, which is generally the case for sandy materials.

The dependence of the maximum tensile strength and degree of saturation on the pore size spectrum parameter n, as described by Eqs. (11) and (12) is shown in Fig. 5. The theory predicts that the normalized maximum tensile strength is a down-and-up function of the n parameter. The corresponding degree of saturation is an increasing function of the n parameter and it can occur at any degree of saturation.

Experimental Validation

Three sands originating from different parts of the world are used for measurement of uniaxial tensile strength, water retention, and shear strength. They are black Esperance sand from Seattle, Washington, clean sand from Perth, Western Australia, and Ottawa sand. The last two sands are commercially available. These sands represent a wide spectrum of particle sizes, particle surface morphologies, and formation environments.

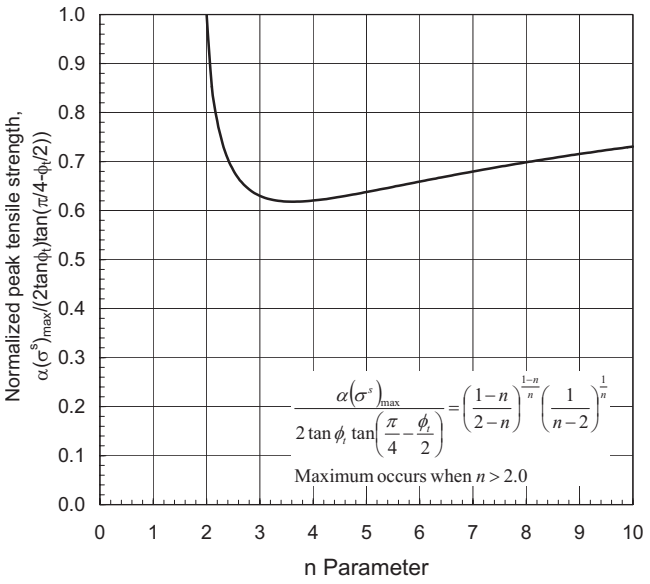

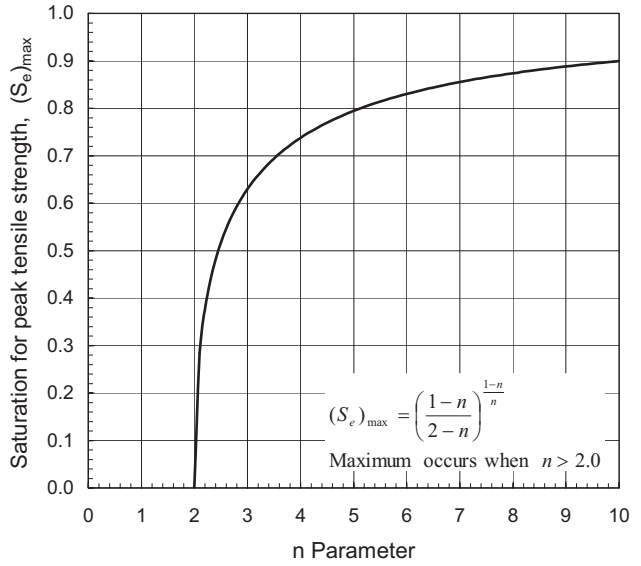

Fig. 5. Theoretical functions for (a) the magnitude of the peak tensile strength as a function of the pore size spectrum parameter n; (b) the equivalent degree of saturation for the peak strength as a function of the pore size spectrum parameter n

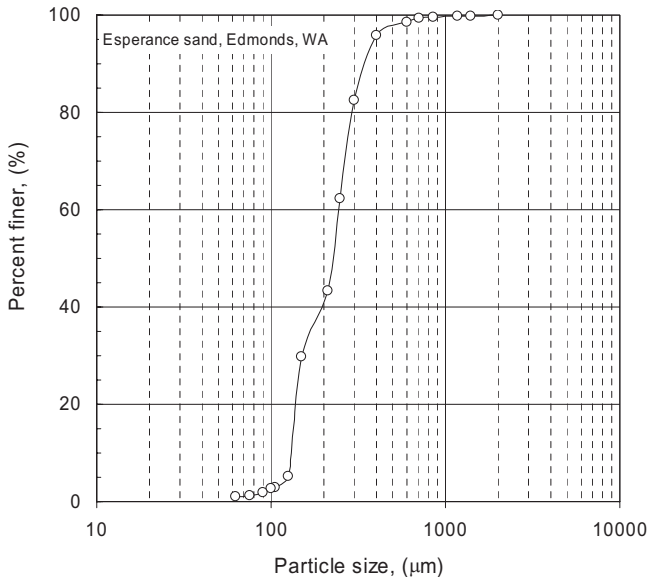

Fig. 6. Particle-size distribution for Esperance sand, from Edmonds, Washington

Esperance Sand

Particle-size distribution of the Esperance sand is shown in Fig. 6. More than 95% of the sand falls within the range of 100–500 μm. The standard Tempe cell is used for soil water retention curve measurement and the result is shown in Fig. 7(a). The residual saturation for this sand is 6.5%. The friction angle at small normal stress level (less than 1 kPa) was determined using a direct shear apparatus modified to accommodate for multistage, constant normal load, and suction control via the hanging column method [Likos et al. (2007). "Modified direct shear apparatus for suction-controlled testing at low stress levels," submitted to *Geotechnical Testing Journal*]. A representative friction angle for stress level less than 1 kPa for the sand with various degrees of saturation is 50°. Uniaxial tensile strength measurements were obtained using the direct tension apparatus described by Lu et al. (2005, 2007). For this sand, measurement of tensile strength at the degree of saturation greater than 93% was not possible as the compaction step in the specimen preparation will liquefy this soil. Tensile strength as a function of the degree of saturation is conducted for this sand compacted at two constant porosity values, 0.4 and 0.45, and the results are plotted in Figs. 7(a and b), respectively. The peak tensile strength is 915 Pa, which occurs around 78% of saturation. The soil water retention curve is governed by Eq. (9) and the uniaxial tensile strength by Eq. (10*b*). The measured soil water retention data are first used to determine parameters α and n and the resulting curve is shown as a dashed curve in Fig. 7(a). For this sand with porosity of 0.40, the best-fit α value is 0.65 kPa^{-1} and n is 3.8. These two parameters, together with the friction angle of 50°, are used in Eq. (10*b*) for tensile strength prediction, as shown as the solid line in Fig. 7. The overall prediction, both in magnitude and the peak strength behavior, follows the experimental data.

For this sand with porosity of 0.45, no attempt is made for the soil water retention measurement. Instead, the measured tensile strength data are used directly to calibrate α and n parameters, which are 0.7 kPa^{-1}, and 4.0, respectively. The same residual saturation of 6.5% is used. These values then are used in Eq. (9) to predict the water retention curve, shown as a dashed curve in Fig. 7(b). The peak tensile strength is 792 Pa around the equivalent degree of saturation compared with this sand with porosity of 0.4, the sand has a smaller air-entry value ($=1/\alpha$ = 1.43 kPa versus 1.54 kPa) as well as slightly wider spectrum of pore sizes (n=4.0 versus 3.8). These are consistent with the fact that this sand has a higher porosity thus lower air-entry pressure and wider pore-size distribution.

Perth Sand

The second type of sand used for the model validation is Perth sand. The complete test results for this sand were reported in Lu et al. (2007). This sand was first sieved and separated to create two distinct subcategories, namely Perth silty sand and Perth medium sand. Particle-size distributions for each of the subcategories are plotted in Figs. 8(a) and 9(a), respectively. This sand has a mean particle size of 105 μm and a narrow spectrum of particle

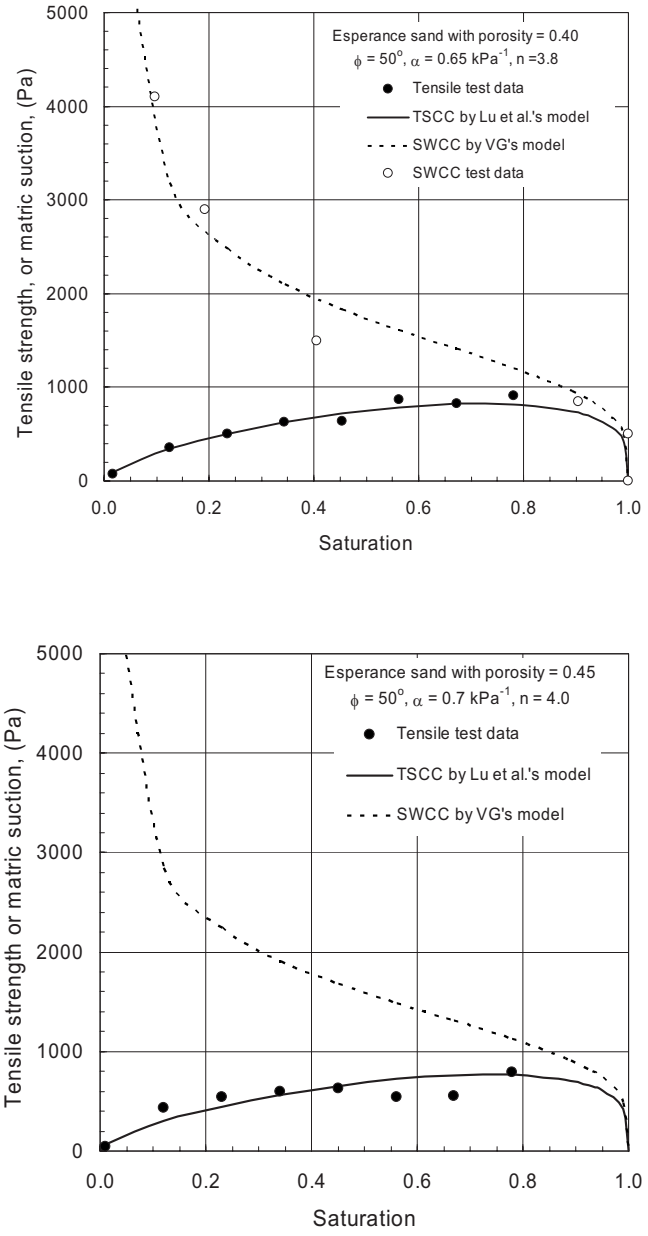

Fig. 7. Comparisons of the measured and predicted soil water retention curve, tensile strength characteristic curve for Esperance sand with porosity of (a) 0.4; (b) 0.45

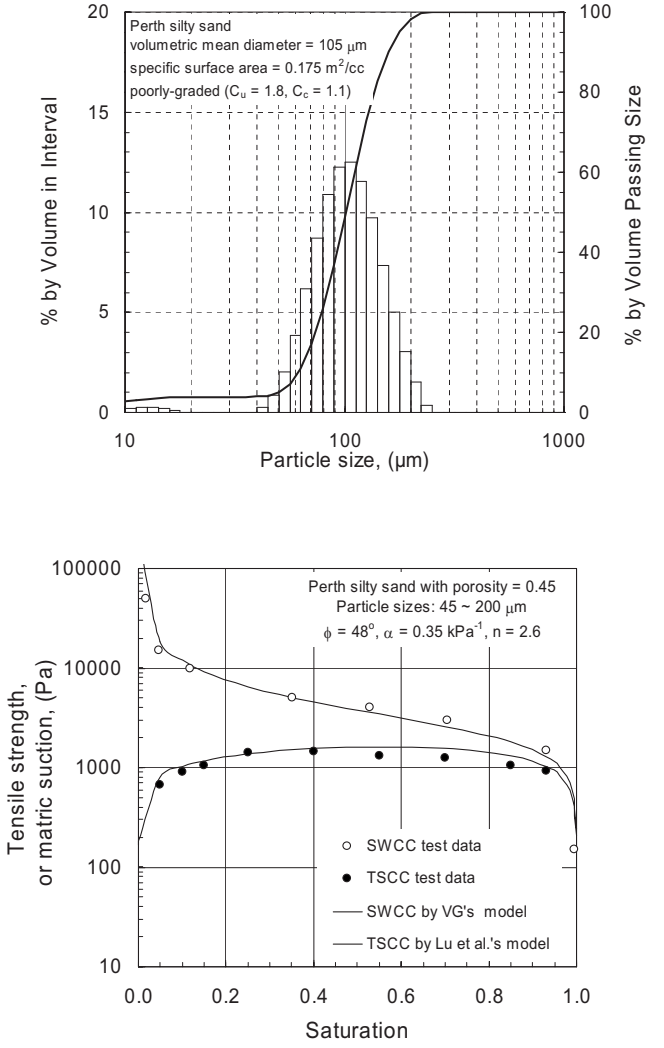

Fig. 8. Experimental validation of tensile strength theory for Perth silty sand: (a) particle-size distribution; (b) experimental data versus theoretical prediction

sizes, ranging from 55 to 200 μm. The mean friction angle at the stress level less than 1 kPa for this sand with various degree of saturation is 48°. The soil water retention curve is measured only for the Perth silty sand using the standard Tempe cell method and the measurements are plotted in Fig. 8(b). The residual degree of saturation is 5.0%. The calibration from the soil water retention yields $\alpha = 0.35$ kPa^{-1} and $n = 2.6$. Tensile strength as a function of the equivalent degree of saturation is measured and plotted in Fig. 8(b). For this soil, tensile strength test can be done at the degree of saturation near 98%. The peak tensile strength of 1,655 Pa at the equivalent degree of saturation 40% is measured. The calibrated α and n parameters, together with the measured friction angle, are used in Eq. (10*b*) to predict the tensile strength shown as a solid curve in Fig. 8(b). As shown, the prediction by Eq. (10*b*) accords well with the measured tensile strength.

The second subcategory of this sand is the Perth medium sand. This soil has a mean particle size of 451 μm and a relatively wide particle sizes, ranging from 200 to 900 μm, as shown in Fig. 9(a). The same residual saturation of 5% is used for calculation. Direct shear tests for various degrees of saturation leads to a mean friction angle of 48°, the same as the Perth silty sand. Tensile strength tests were conducted under two distinct porosity values, 0.37 and 0.40, and the results are plotted together in Fig. 9(b). The peak tensile strength for the sand with porosity 0.37 is 810 Pa at the equivalent degree of saturation 90% while the peak tensile strength for the sand with porosity of 0.40 is 744 Pa at the equivalent degree of saturation 70%. In general these two soils have very similar tensile strength behavior. Tensile strengths for both porosities are used together to calibrate α and n parameters. The calibrated α is 0.8 kPa^{-1} and n is 4.0. Compared to the Perth silty sand, the medium sand has much smaller peak tensile strength (average 777 Pa for the medium sand versus 1,655 Pa for the silty sand), less air-entry pressure (1.43 kPa versus 2.86 kPa), and wider particle sizes ($n = 4.0$ versus 2.6). The predicted tensile strength peaks at 750 Pa with 79%, agreeing well with the average values for this sand.

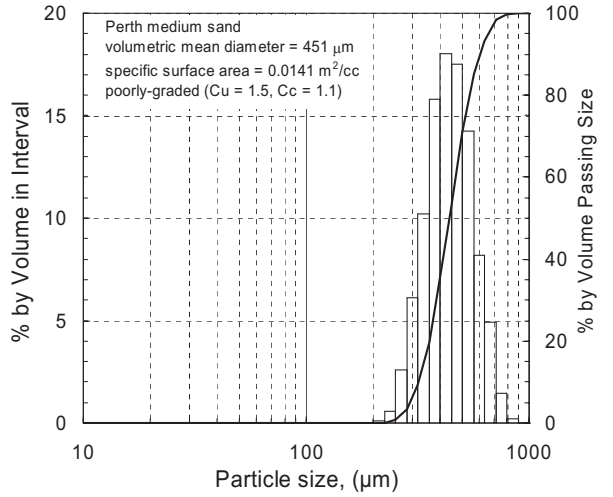

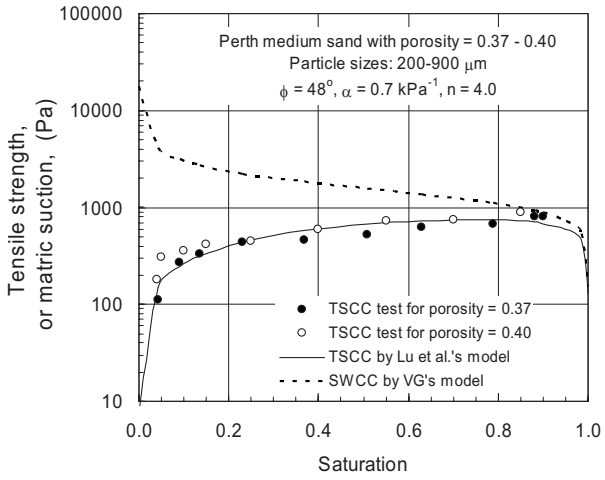

Fig. 9. Experimental validation of tensile strength theory for Perth medium sand: (a) particle-size distribution; (b) experimental data versus theoretical prediction

Ottawa Sand

The third type of sand is Ottawa sand (C-75). The particle-size distribution is shown in Fig. 10. Two subcategories of this sand are created: one is washed through a #200 sieve (0.075 mm) to remove fines and the other is prepared by adding 2% of those fines. Both soils were prepared to a constant relative density of 50% or porosity of 0.39. SWCC were measured by Hwang (2002) using a flow pump technique developed by Znidarčić et al. (1991). Shear strength of unsaturated sand is measured by a special direct shear box with dimensions of $178 \times 178 \times 15$ mm (Perkins 1991; Kim 2001), which is capable of normal stress measurement as low as 100 Pa. Tensile strength tests are conducted by an apparatus modified from the original version of Perkins (1991). The specimen container ($178 \times 178 \times 178$ mm) is split in two equal halves (Kim 2001).

The average friction angle for various degrees of saturation is 55° for the smallest stress range between 0.1 and 0.25 kPa. The measured soil water retention data for the clean Ottawa sand are plotted in Fig. 11(a). The measured residual saturation is 15%. The measured tensile strength data for the clean Ottawa sand (F-75-C) are plotted in Fig. 11(a) and the tensile strength for the Ottawa sand (F-75-F) with fines are plotted in Fig. 11(b). The

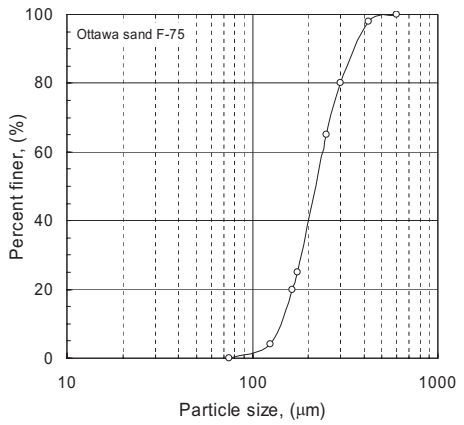

Fig. 10. Particle-size distribution for Ottawa sand

measured peak tensile strength for F-75-C is 1,598 Pa at 61% saturation, and for F-75-F is 1,527 at 59%. The measured soil water retention data are used to calibrate α and n parameters, which are 0.41 kPa^{-1} and 2.9, respectively. The predicted tensile strength characteristic curve, using the calibrated parameters, is plotted as the solid curve in Fig. 11(a). Both the predicted peak tensile strength (1,395 Pa) and the corresponding degree of satu-

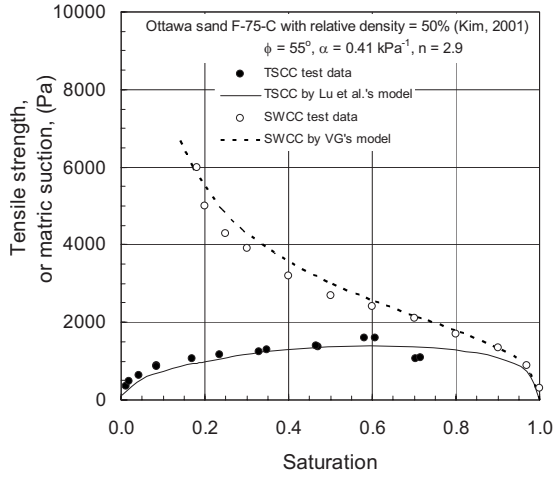

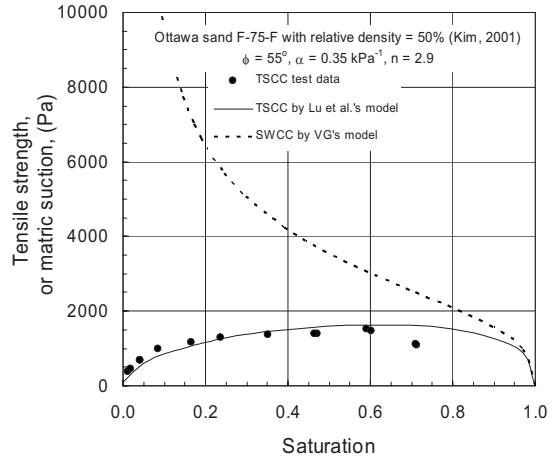

Fig. 11. Experimental validation of tensile strength theory for Ottawa sand: (a) F-75 with no fines; (b) F-75 with 2% fines

ration (59.6%), as well as the overall trend, accord reasonable well (12.5% relative error) with the measured data.

For F-75-F sand, the calibrated tensile strength characteristic curve is obtained by directly using the measured tensile strength data, as shown in Fig. 11(b). The predicted peak tensile strength is 1,635 Pa occurring at the equivalent degree of saturation 59.6%, whereas the measured peak tensile strength is 1,529 Pa occurring at the equivalent degree of saturation 59.1%, showing that the relative error for tensile strength is less than 7%. Compared to F-75-C sand, this soil shows slightly higher air-entry pressure (2.86 kPa for F-75-F versus 2.34 kPa for F-75-C) but with identical pore size spectrum number ($n=2.9$).

In summary of the experimental validation, the proposed theory for tensile strength can predict accurately the variation of tensile strength pattern in all three water retention regimes, its peak values, and the occurrence of the peak strength.

Summary and Conclusions

A theory that accurately describes tensile strength of moist sand is presented. The theory is based on a generalized effective stress for variably saturated soil proposed earlier by Lu and Likos (2004,2006). The interparticle stress called suction stress is identified in place of pore water pressure in Terzaghi's effective stress. In general, suction stress has four components that originate from different water retention mechanisms: van der Waals attraction, electric double layer forces, tensile pore water pressure, and surface tension. In the case of sand, interparticle stresses due to the first two mechanisms can be safely ignored and capillary stress is the major reason for sand to exhibit cohesiveness. In formulating and identifying suction stress, Lu and Likos (2006) suggested the isotropic tensile strength projected from a linear extension of the M-C failure criterion can be directly used. Using existing unsaturated shear strength data for silty and clayey soil, Lu and Likos (2006) demonstrated that the isotropic tensile strength can unify shear strength behavior under various suction conditions onto the simple M-C criterion. The linear shear strength assumption works well there because the stress level involved in many lab and field conditions is on the order of several tens to high hundreds of kPa and shear strength behavior within this range can be practically represented by the M-C criterion.

For most soil under small stress level less than several kPa, nonlinear yield behavior becomes evident; the internal friction angle generally increases significantly as the normal stress decreases and dry sand can often exhibit apparent cohesion due to interlocking among soil grains. This is particularly true for sand. The stress range for the nonlinear behavior also coincides with the magnitude of the capillary stress commonly encountered in unsaturated sand. Many field geomechanical problems also operate within this stress range. Thus it is important to develop a more accurate and representative suction stress under such environments. The theory presented in this paper proposes a more accurate way to identify isotropic tensile strength and uniaxial tensile strength by explicitly considering the nonlinear nature of the failure envelope at low stress level and capillary stress within all three water retention regimes, namely pendular, funicular, and capillary. A closed form expression for tensile strength unifies tensile strength characteristics in all three water retention regimes. Tensile strength of sand characteristically varies with either saturation or soil suction in an up-and-down manner with a peak tensile strength that can occur at any degree of saturation. Three parameters are employed in the theory, namely, the internal friction angle (at low normal stress) ϕ_f, the inverse value of the air-entry pressure α, and the pore size spectrum parameter n. The last two parameters are identical to the widely recognized soil water retention model defined by van Genuchten (1980). It is shown that the magnitude of the peak tensile strength is dominantly controlled by the α parameter, where as the saturation at which the peak tensile strength occurred only depends on the pore size spectrum parameter n.

Three sands with different particle-size distributions are used to validate the proposed theory. The closed form expression accords well with the experimental data obtained from these sands in terms of the variation patterns of tensile strength over the entire saturation regimes, the magnitudes of the tensile strength, it peak value, and the corresponding degree of saturation when the peak strength occurs.

Because the fact that the theory considers isotropic tensile strength as suction stress that generalizes Terzaghi's effective stress to variably saturated soil, experimental validation shown here is another vindication of the validity of suction stress characteristic curve in describing stress behavior. The generalized effective stress for variably saturated sandy soil is completely defined by Eqs. (3), (6), and (7). This work also demonstrates that stress due to interparticle forces (isotropic tensile stress) and soil water retention in sand share some common fundamental control: pore size distribution, which can be fully described by the same parameters α and n.

Acknowledgments

This research is partially funded by a grant from American Chemical Society (ACS-PRF 42688–A9) to the senior writer.

References

Al-Hussaini, M. M., and Townsend, F. C. (1974). "Tensile testing of soils: A literature review." *Rep. No. S-74-10*, U.S. Army Waterways Experiment Station, Vicksburg, Miss.

Bishop, A. W., and Garga, V. K. (1969). "Drained tests on London clay." *Geotechnique*, 19(2), 309–312.

Blight, G. E. (1967). "Effective stress evaluation for unsaturated soils." *J. Soil Mech. and Found. Div.*, 93(2), 125–148.

Cho, G. C., and Santamarina, J. C. (2001). "Unsaturated particulate materials: Particle-level studies." *J. Geotech. Geoenviron. Eng.*, 127(1), 84–96.

Dallavalle, J. M. (1943). *Micrometrics*, Pitman, London.

Fisher, R. A. (1926). "On the capillary forces in an ideal soil: Correction of formula given by W. B. Haines." *J. Agric. Sci.*, 16, 492–505.

Hwang, C. S. (2002). "Determination of material functions for unsaturated flow." Ph.D. thesis, Univ. of Colorado at Boulder, Colo.

Ingles, O. G. (1962). "Bonding forces in soils. Part III: A theory of tensile strength for stabilized and naturally coherent soils." *Proc., 1st Conf. of the Australian Road Research Board*, 1025–1047.

Kim, T.-H. (2001). "Moisture-induced tensile strength and cohesion in sand." Ph.D. thesis, Dept. of Civil, Environmental and Architectural Engineering, Univ. of Colorado, Boulder, Colo.

Kim, T.-H., and Hwang, C. (2003). "Modeling of tensile strength on moist granular earth material at low water content." *Eng. Geol. (Amsterdam)*, 69, 233–244.

Likos, W. J., and Lu, N. (2004). "Hysteresis of capillary stress in unsaturated granular soil." *J. Eng. Mech.*, 130(6), 646–655.

Lu, N., and Likos, W. J. (2004). *Unsaturated soil mechanics*, Wiley, New York.

Lu, N., and Likos, W. J. (2006). "Suction stress characteristic curve for

unsaturated soil." *J. Geotech. Geoenviron. Eng.*, 132(2), 131–142.
Lu, N., Wu, B., and Tan, C. P. (2005). "A tensile strength apparatus for cohesionless soils." *Proc., Experus 2005*, A. Tarantino, E. Romero, and Y. J. Cui, eds., Balkema, Rotterdam, The Netherlands.
Lu, N., Wu, B., and Tan, C. P. (2007). "Tensile strength characteristics of unsaturated sands." *J. Geotech. Geoenviron. Eng.*, 133(2), 144–154.
Maksimovic, M. (1989). "Nonlinear failure envelope for soils." *J. Geotech. Engrg.*, 115(4), 581–586.
Maksimovic, M. (1996). "A family of nonlinear failure envelopes for non-cemented soils and rock discontinuities." *Electron. J. Geotech. Engrg.*, 1, 1–36.
Mehrotra, V. P., and Sastry, K. V. S. (1980). "Pendular bond strength between unequal-sized particles." *Powder Technol.*, 25, 203–214.
Perkins, S. W. (1991). "Modeling of regolith structure interaction on extraterrestrial constructed facilities." Ph.D. thesis, Univ. of Colorado, Boulder, Colo.
Rumpf, H. (1961). "The strength of granules and agglomerates." *Agglomeration*, W. A. Knepper, ed., Interscience, New York.
Schubert, H. (1982). *Kapillarität in porösen festsoffsystemen*, Springer, Berlin.
Sparks, A. D. W. (1963). "Theoretical considerations in stress equations for partly saturated soils." *Proc., 3rd Regional Conf. for Africa on Soil Mechanics*, Salisbury, Rhodesia, 215–218.
Sture, S., et al. (1998). "Mechanics of granular materials at low effective stresses." *J. Aerosp. Eng.*, 11(3), 67–72.
van Genuchten, M. T. (1980). "A closed form equation for predicting the hydraulic conductivity of unsaturated soils." *Soil Sci. Soc. Am. J.*, 44, 892–898.
Zeh, R. M., and Witt, K. J. (2007). "The tensile strength of compacted clays as affected by suction and soil structure." *Experimental unsaturated soil mechanics*, T. Schanz, ed., Springer, New York, 219–226.
Znidarcic, D., Illangasekare, T., and Manna, M. (1991). "Laboratory testing and parameter estimation for two-phase flow problems." *Geotech. Spec. Publ.*, 27, 1089–1099.